Supplementary information for
Spin injection through energy-band symmetry matching with high spin polarization in atomically controlled ferromagnet/ferromagnet/semiconductor structures

Michihiro Yamada,[†] Fumiaki Kuroda,[‡] Makoto Tsukahara,[†] Shinya Yamada,[†] Tetsuya Fukushima,[†,¶,§] Kentarou Sawano,[‖] Tamio Oguchi,[†,⊥,#] and Kohei Hamaya[*,†]

†*Center for Spintronics Research Network, Graduate School of Engineering Science, Osaka University, 1-3 Machikaneyama, Toyonaka 560-8531, Japan.*

‡*Department of Material Engineering Science, Graduate School of Engineering Science, Osaka University, 1-3 Machikaneyama, Toyonaka 560-8531, Japan.*

¶*Institute for NanoScience Design, Osaka University, Toyonaka 560-8531, Japan.*

§*Institute for Datability Science, Osaka University, Suita 565-0871, Japan.*

‖*Advanced Research Laboratories, Tokyo City University, 8-15-1 Todoroki, Tokyo 158-0082, Japan.*

⊥*Institute of Scientific and Industrial Research, Osaka University, Ibaraki 567-0047, Japan.*

#*MaDIS, National Institute for Materials Science, Tsukuba 305-0047, Japan.*

E-mail: hamaya@ee.es.osaka-u.ac.jp

S1: $J - V$ measurements for FM/Ge contacts

Current density – voltage ($J - V$) characteristics for FM/Ge contacts, i.e., CFAS/Ge with or without inserting Fe atomic layers, in all the LSV devices were measured by the three-terminal measurements, as shown in Fig. S1(a). Here V_{int1} or V_{int2} stands for the bias voltage applied to the FM1/SC or FM2/SC interfaces, respectively, as shown in Fig. S1(a). In this study, the conditions of $V_{\mathrm{int1}} < 0$ were used as spin-injection conditions of electrons from CFAS to Ge. All the data at 8 K were shown in Fig. S1(b). Since the two δ-doped layers (δ-P + Si) were introduced between CFAS and Ge,[1] all the $J - V$ characteristics of the CFAS/Ge contacts in LSV devices were governed by the Schottky-tunnel barriers and did not depend on the number of the inserted Fe atomic layers.

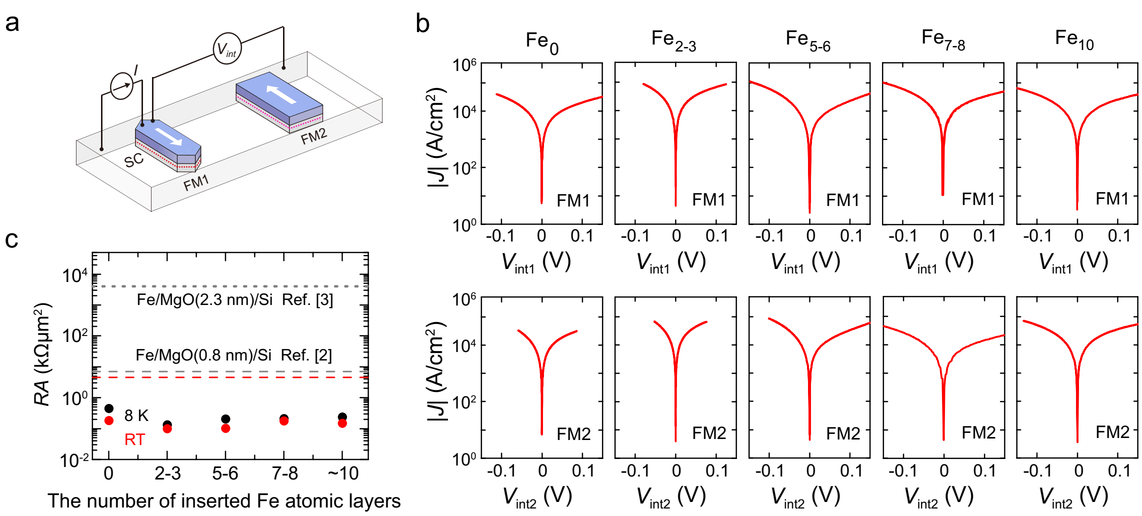

Figure S 1: (a) Schematic of a FM-SC-FM lateral spin-valve (LSV) device, in which terminal configurations of three-terminal voltage measurements for $J - V$ characteristics are drawn. (b) $J - V$ characteristics of all the contacts with and without inserting Fe atomic layers at 8 K. (c) Variation in the RA values of the FM/SC contacts by controlling the number of the inserted Fe atomic layers at 8 K (black) and room temperature (red). The red and gray dashed lines are reference values for Fe/MgO/Si contacts[2,3] at 8 or 10 K and room temperature, respectively.

As summarized in Fig. S1(c), the value of RA at the spin-injection condition is kept to be less than 0.40 k$\Omega\mu$m^2, maintaining the low parasitic resistance at the electrodes. Note that the value of RA in this study is one or two orders of magnitude lower than those in

Fe/MgO(0.8 nm)/Si contacts.[2] Recently, although a very large tunnel spin polarization of 90 % at 10 K was reported in Fe/MgO(2.3 nm)/Si,[3] the value of RA was three orders of magnitude larger than those in this study.

S2: Spin diffusion length of the used n-Ge channel

In the nonlocal measurement setups shown in Fig. 1(a), we can also estimate the spin diffusion length (λ_{N}) of the used n-Ge channel layers. When we applied out-of-plane magnetic field (B_{z}) to the LSV devices under the parallel and antiparallel magnetization configurations to record ΔR_{NL} as functions of B_{z}, we also observed evident Hanle-type spin precession curves, indicating the generation, manipulation, and detection of spin currents in the n-Ge layer by all electrical means, in the nonlocal measurements, as shown in Fig. S2.

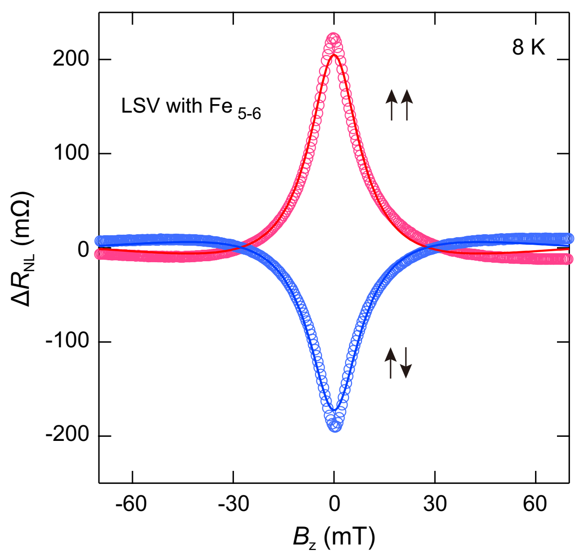

Figure S 2: Nonlocal Hanle signals for an LSV device with Fe_{5-6} at 8 K. The solid curves are fitting results using Eq. (S1).

These data are evidence for the reliable spin transport in the used semiconductor, demonstrated by electrical spin injection and detection.[4,5] Using the Hanle curves, we can roughly extract spin lifetime (τ_{N}) and the diffusion constant (D) values in n-Ge. According to the previous works,[4] the nonlocal Hanle curves are expressed as the following one dimensional spin drift diffusion model,

$$\Delta R_{\mathrm{NL}}(B_{\mathrm{z}}) = \pm A \int_{0}^{\infty} \phi(t) \cos(\omega_L t) \exp\left(-\frac{t}{\tau_{\mathrm{N}}}\right) dt, \tag{S1}$$

where $A = \frac{P^2 \rho_{\mathrm{N}} D}{S}$, $\phi(t) = \frac{1}{\sqrt{4\pi D t}} \exp\left(-\frac{L^2}{4Dt}\right)$, ω_L $(= g\mu_{\mathrm{B}} B_z/\hbar)$ is the Larmor frequency, g is the electron g-factor (g = 1.56) in Ge,[1] and μ_{B} is the Bohr magneton. Here, ρ_{N} is the resistivity of n-Ge (1.59 mΩcm $\leq \rho_{\mathrm{N}} \leq$ 2.16 mΩcm), S is the cross section ($S = 0.98$ μm^2) of the n-Ge layer used here, and L is the center-to-center distance between the spin injector and detector (L = ∼0.9 μm). From this Hanle analysis, we can also obtain λ_{N} from the relation, $\lambda = \sqrt{D\tau}$. As a result, we can clearly obtain almost no dependence of the number of the inserted Fe atomic layers on λ_{N} (λ_{N} = 0.84 ±0.07 μm).[6] Therefore, there is no influence of the insertion of the Fe atomic layers between CFAS and Ge on the spin transport in the used n-Ge layer.

S3: Electronic band structure at CFAS/Fe/Ge interfaces

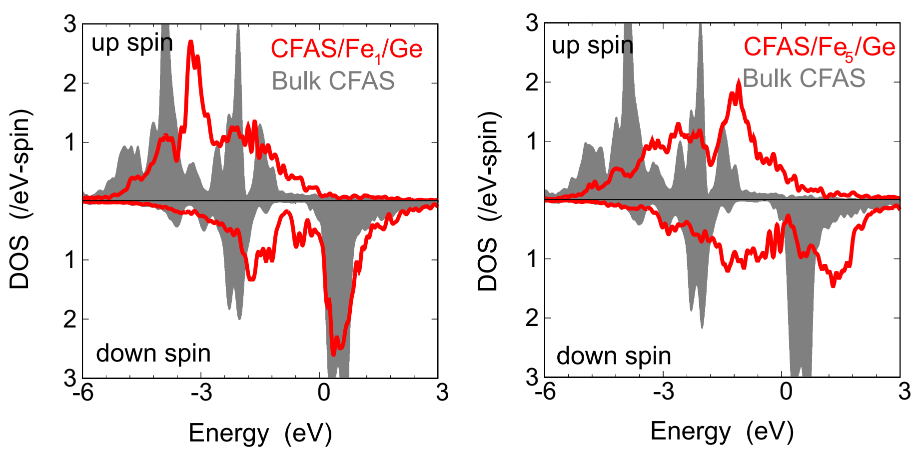

Figure S 3: Calculated density of states for d electrons of interfacial Fe (red) for CFAS/Fe_1/Ge and CFAS/Fe_5/Ge interfaces, together with that of bulk Fe for CFAS (gray).

The electronic structures of the CFAS/Fe_1/Ge and CFAS/Fe_5/Ge interfaces are checked theoretically. Figure S3 shows the partial density of states (PDOS) of the CFAS/Fe_1/Ge and CFAS/Fe_5/Ge, obtained from first-principles density-functional theory calculations.[7,8]

For interfacial Fe of both CFAS/Fe_1/Ge and CFAS/Fe_5/Ge heterojunctions, both the up-spin and down-spin d states near the Fermi level are significantly changed, giving rise to the low spin polarization (red). Thus, from the viewpoint of the PDOS, we can theoretically understand that the CFAS/Fe_1/Ge and CFAS/Fe_5/Ge interfaces are not useful to obtain highly efficient spin injection.

S4: Magnetoresistance ratio at 8 K

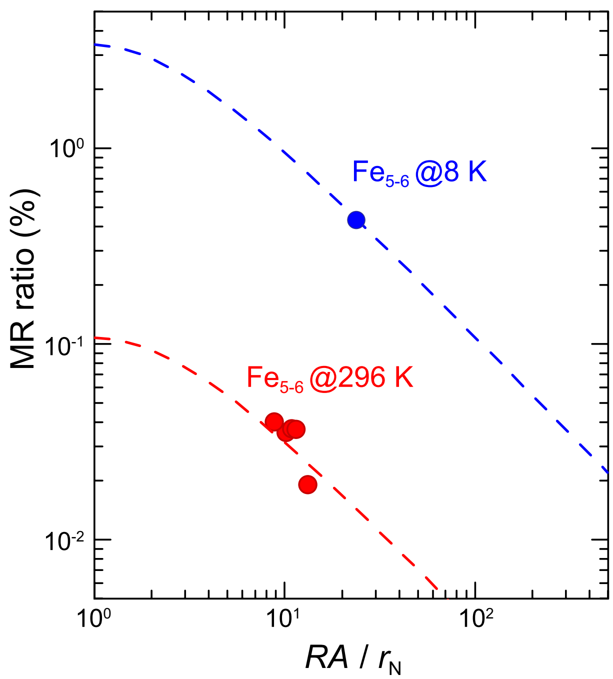

Figure S 4: MR ratio (%) for LSV devices with Fe_{5-6} at 8 K (blue), together with the data at 296 K (red) shown in Fig. 6 c. The value of r_N is the spin resistance of the spin-transport layers, where r_N = 10.6 $\Omega\mu m^2$ at 8 K for the n-Ge used here. The blue dashed curve is a guide line based on the standard theory with $\gamma = 0.425$.[9]

Magnetoresistance (MR) ratio for LSV devices with Fe_{5-6} at 8 K is plotted in Fig. S4, together with those at 296 K. The MR ratio at 8 K is enhanced up to 0.43 %, which is one order of magnitude larger than those at 296 K because of the increase in the interface spin polarization (γ) and spin diffusion length (λ_N) of n-Ge at 8 K.

References

1. Hamaya, K. et al. Spin transport and relaxation in germanium. *J. Phys. D: Appl. Phys.* **51**, 393001 (2018).

2. Suzuki, T. et al. Room-Temperature Electron Spin Transport in a Highly Doped Si Channel. *Appl. Phys. Express* **4**, 023003 (2011).

3. Spiesser, A., Saito, H., Yuasa, S. & Jansen, R. Tunnel spin polarization of Fe/MgO/Si contacts reaching 90% with increasing MgO thickness. *Phys. Rev. B* **99**, 224427 (2019).

4. Lou, X. et al. Electrical detection of spin transport in lateral ferromagnet–semiconductor devices. *Nat. Phys.* **3**, 197–202 (2007).

5. Appelbaum, I., Huang, B. & Monsma, D. J. Electronic measurement and control of spin transport in silicon. *Nature* (London) **447**, 295-298 (2007).

6. Yamada, M. et al. Large impact of impurity concentration on spin transport in degenerate *n*-Ge. *Phys. Rev. B* **95**, 161304(R) (2017).

7. Giannozzi, P. et al. QUANTUM ESPRESSO: a modular and open-source software project for quantum simulations of materials. *J. Phys.: Condens. Matter.* **21**, 395502 (2009).

8. Perdew, J. P., Burke, K. & Ernzerhof, M. Generalized Gradient Approximation Made Simple. *Phys. Rev. Lett.* **77**, 3865–3868 (1996).

9. Jaffrès, H., George, J.-M. & Fert, A. Spin transport in multiterminal devices: Large spin signals in devices with confined geometry. *Phys. Rev. B* **82**, 140408(R) (2010).